Camera / System Calibration of LiDAR-Vision Sensor Module Mounted on A Ground Disaster Investigation Robot

Kim S.S. [1*], Jung Y.H.[2], Lim E.T.[2] and Koo S.[2]

[1]Research officier, Disaster Scientific Investigation Div., National Disaster Management Research Institute, Rep. of Korea

[2]Researcher, Disaster Scientific Investigation Div., National Disaster Management Research Institute, Rep. of Korea

*sskim73@korea.kr

ABSTRACT

The camera and system calibration process is an essential pre-processing step for ensuring the accuracy of the LiDAR/Vision-based Simultaneous Localization and Mapping (SLAM) module. Firstly, camera calibration estimates the interior orientation parameters (IOPs). Additionally, system calibration calculates the relative positions and attitudes of individual sensors which constitute the multi-sensor module of the investigation robot, geometrically enhancing the overall observation accuracy of the system. Experiments for camera and system calibration were conducted by placing wall targets and V-shaped three-dimensional calibration boards in indoor spaces and acquiring images and point clouds for various experimental conditions. Considering the field of view between the camera and LiDAR, camera resolution, distance, and indoor illumination, the characteristics of noise generation in the LiDAR point cloud were confirmed. For system calibration of the multi-sensor module, images and point clouds for the V-shaped three-dimensional calibration board were obtained from 9 locations at a rate of 20 shots per second, while for camera calibration, image data for flat calibration boards on walls were obtained from 6 locations, considering distance and height variations. The results of camera and system calibration showed precise experimental outcomes, with the camera IOP estimation error (RMSE) through the calibration experiment being 0.39 pixels and the system calibration between LiDAR and camera showing errors within 0.2 pixels. Based on the experimentally derived system and camera calibration results, it is anticipated that the enhanced SLAM accuracy of future investigation robots in indoor spaces and more precise and accurate detection and analysis of indoor disaster information could be achieved.

Keywords: Disaster scene investigation, ground robot, camera calibration, system calibration

1. Introduction

The increasing frequency and severity of natural disasters, driven by climate change and extreme weather events, have led to significant damage globally. The Korean Peninsula, located on Northeast Asia, has also experienced unprecedented weather conditions, particularly during the monsoon season of 2023. Record-breaking rainfall, including

intense downpours exceeding 100mm per hour, caused severe flooding, landslides, and other disasters, resulting in substantial human and property losses. Over 90 casualties, the flooding of 36,865.6 hectares of farmland, and damage to more than 13,884 facilities were reported during this period alone (Wikipedia, 2023).

In response to such catastrophic events, the National Disaster Management Research Institute (NDMI) has been leveraging advanced technologies such as drones, robots, and specialized vehicles for disaster site monitoring, data collection, and decision-making support. Since 2021, the NDMRI has been developing technologies for using ground disaster investigation robots, such as the iRobot Packbot, in scenarios where human access is difficult, including earthquake-affected and collapsed structures (NDMI 2022, NDMI 2023).

Parallel to these advancements, the field of geo-spatial information has seen a surge in research focused on integrating the latest terrain observation sensors. The rapid development of high-resolution cameras, LiDAR systems, and mobile mapping platforms, including drones and robots, has made it easier to quickly and accurately acquire high-precision spatial data in both indoor and outdoor environments. These mobile sensing and mapping platforms are equipped with a variety of sensors, such as cameras and laser scanners, that are synchronized and integrated to efficiently collect disaster site data. With the integration of cutting-edge technologies like deep learning, digital twins, the Internet of Things (IoT), edge/fog cloud computing, and high-speed data transmission, these platforms are continuously evolving.

Building upon these technological advancements, this paper presents a method for calibrating the camera and overall system of a multi-sensor module mounted on a ground disaster investigation robot. The calibration process for the investigation robot platform was conducted in two stages: camera calibration and system calibration. In the camera calibration stage, the interior orientation parameters (IOPs) and lens distortion variables of the cameras within the multi-sensor module were calculated. This involved establishing a mathematical model that relates numerous 2D points in the camera images to their corresponding 3D real-world coordinates, thereby determining the internal and external orientation parameters of the camera.

In the subsequent system calibration stage, the relative orientation parameters (ROPs) between the sensors were estimated to define the relative geometric positions and attitudes of the sensors. This involved constructing a sensor bundle with the camera and LiDAR, given their high field-of-view (FOV) overlap, and then performing system calibration to

estimate the relative positions and attitudes. The calibration was carried out using a point-plane correspondence-based approach, which imposes the condition that "all points extracted from the camera images must lie on the same plane as those extracted from the LiDAR point cloud." This process improves the alignment accuracy between the point cloud data and the camera's RGB information, ultimately enhancing the performance of the integrated sensor module and the mapping accuracy of the Vision-LiDAR SLAM system.

2. Methodology

2.1 Theoretical Background of Camera Calibration

Camera calibration determines the interior orientation parameters (IOPs) and exterior orientation parameters (EOPs) of the camera sensor in the multi-sensor module. This process corrects the distortions and errors in the images caused by camera lens distortion. Once these distortions and errors in the captured images are corrected, the corresponding RGB information from the LiDAR point cloud data can be accurately registered with the camera images in the multi-sensor module. The intrinsic parameters of the camera calibration include the camera's focal length, the position of the principal point representing the center of the camera image, radial lens distortion, decentering lens distortion, and affine distortion. The extrinsic orientation parameters of the camera calibration include the camera's position(X_0, Y_0, Z_0) and orientation (ω, φ, κ).

The camera model, known as the collinearity condition, which states that the principal point of the camera (x_p, y_p), the image coordinates (x, y), and an arbitrary point (X_A, Y_A, Z_A) in 3D space must lie on the same straight line, can be expressed as follows. The extended collinearity model within a bundle adjustment, incorporating self-calibration is defined as:

$$x_a = x_p - c\frac{r_{11}(X_A - X_o) + r_{12}(Y_A - Y_o) + r_{13}(Z_A - Z_o)}{r_{31}(X_A - X_o) + r_{32}(Y_A - Y_o) + r_{33}(Z_A - Z_o)} + \Delta x \quad (1)$$

$$y_a = y_p - c\frac{r_{21}(X_A - X_o) + r_{22}(Y_A - Y_o) + r_{23}(Z_A - Z_o)}{r_{31}(X_A - X_o) + r_{32}(Y_A - Y_o) + r_{33}(Z_A - Z_o)} + \Delta y \quad (2)$$

The distortion amount ($\Delta x, \Delta y$) of the image coordinates is calculated using the following equations:

$$\Delta x = \bar{x}(K_1 r^2 + K_2 r^4 + K_3 r^6) + P_1(r^2 + 2\bar{x}^2) + 2P_2\bar{x}\bar{y} + A_1\bar{x} + A_2\bar{y} \quad (3)$$

$$\Delta y = \bar{y}(K_1 r^2 + K_2 r^4 + K_3 r^6) + P_2(r^2 + 2\bar{y}^2) + 2P_1 \bar{x}\bar{y} \quad (4)$$

where (K_1, K_2, K_3) represents radial distortion, (P_1, P_2) represents decentering distortion, and (A_1, A_2) represents affine distortion. Additionally, ($\bar{x}, \bar{y}$) are the corrected image coordinates at the principal point, as shown in the following equations:

$$\bar{x} = x - x_p \quad (5)$$

$$\bar{y} = y - y_p \quad (6)$$

The final corrected image coordinates (*x*, *y*) are then computed using the following equations (Choi *et al*. 2019, Choi and Kim, 2021).

$$x = x_p - \frac{r}{\sqrt{U^2 + V^2}} U + \Delta x \quad (7)$$

$$y = y_p - \frac{r}{\sqrt{U^2 + V^2}} V + \Delta y \quad (8)$$

2.2 Multi-Sensor Module Development and Specifications

The investigation robot platform under development in this study is equipped with a multi-sensor module consisting of a camera, IMU, and LiDAR for indoor and outdoor site investigations in disaster areas (Figure 1). The main specifications of each sensor are listed in Table 1.

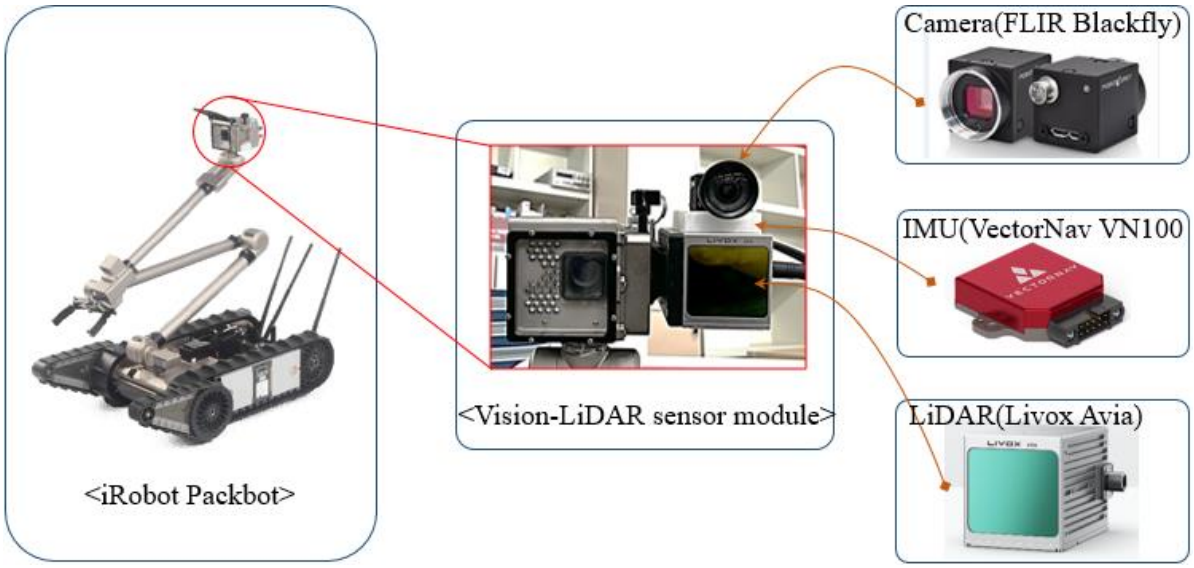

Figure 1. Multi-sensor module configuration of the investigation robot platform

Table 1. Key specification for each sensor in the multi-sensor module

Devices	Model	Specification
EO camera	FLIR Blackfly	Resolution: 1280×1024, Image pixel: 1.3MP, Frame rate: 170fps, Focal length: 4mm
IMU	VectorNavVN100	Gyroscope: 5°/hr/√Hz, Accelerator: 0.04mg/√Hz, Magnetometer:140μGauss/√Hz
LiDAR	Livox Avia	Hor. FoV: 70.4° / Ver. FoV: 77.2°, Range: Max. 450m, Accuracy: < 2 ㎝

2.3 Suggested Methodology for Calibration of the Multi-sensor Module

The calibration of the investigation robot's multi-sensor module was conducted in two stages: camera calibration and system calibration. In the first stage, camera calibration was performed to estimate the camera's intrinsic orientation parameters, followed by image correction. In the second stage, system calibration was conducted to accurately calculate the relative pose information (position, orientation) between the camera and LiDAR sensors. After system calibration, the RGB information from the camera was accurately registered with the LiDAR point cloud data to generate a point cloud with RGB values. The process is illustrated in Figure 2.

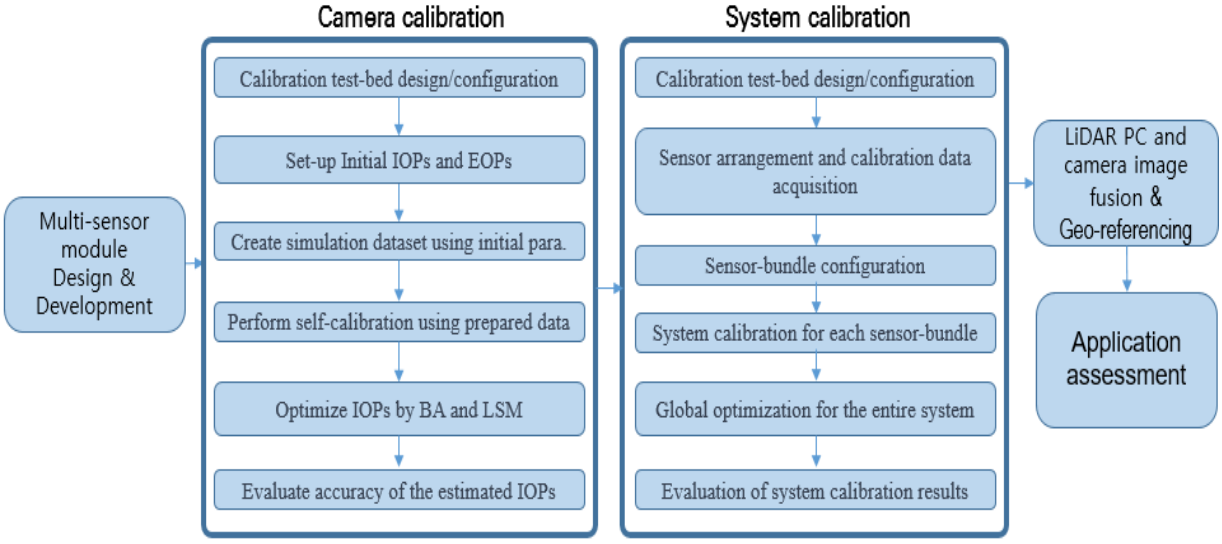

Figure 2. System calibration flowchart for multi-sensor module of the investigation robot

3. Experimental Results and Discussion

3.1 Setting-up of Calibration Experiment Environment and Data Acquisition

The camera calibration experiment was conducted in a test-bed located within the 4th Engineering Building at Myongji University's Natural Science Campus. The test-bed consists of a vertical wall measuring 6.5 meters in the X-axis direction, 5.5 meters in the Z-axis direction, and 2.5 meters in height (Y-axis direction), with 40 targets (arranged in 5 rows by 8 columns) attached to the wall (Figure 3). The camera used for this experiment was the FLIR Blackfly digital camera, which is part of the multi-sensor module mounted on the survey robot. According to the manufacturer's specifications, the focal length (f) of the camera is 4 mm, with an image size of 1,280 × 1,024 pixels, a sensor size of 6.144 mm × 4.9152 mm, and a pixel size of 0.0048 mm.

For system calibration, the test-bed was constructed by placing seven V-type stereoscopic targets (100 cm × 60 cm) in front of the vertical wall (6.5 m × 5.5 m × 2.5 m (H)) (Figure 3). The equipment used for system calibration included the FLIR Blackfly digital camera and the Livox Avia LiDAR sensor, both of which are mounted on the survey robot's multi-sensor module. The horizontal field of view (FoV) of both the Livox Avia LiDAR sensor and the FLIR Blackfly camera is approximately 70˚, providing nearly identical characteristics.

Figure 3. Calibration test-bed of investigation robot (left: camera clibration, right: system calibration)

For the camera calibration data, images were taken at six points (F1~F6) targeting the vertical wall targets, with the camera positioned in a forward direction (κ=0˚) and rotated 90˚ clockwise (κ=90˚) (Figure 4). A total of 12 images were used for camera calibration.

Figure 4. Camera calibration targets on test-bed wall (left: κ=0°, right: κ=90°)

The system calibration experiment data was acquired by photographing two types of images at nine points (E1~E9) with different camera heights (65 cm, 150 cm, repectively) using the V-type stereoscopic targets. LiDAR data (point cloud data, *.pcd, 10 Hz/sec.) was also collected, resulting in 18 images and LiDAR point clouds, which were used for camera calibration (Figure 5).

Figure 5. V-type targets setting-up for system calibration (left: 150cm height, right: 65cm height)

3.2 Camera Calibration Experimental Results

As mentioned earlier, the digital camera used in this experiment was the FLIR Blackfly, with a focal length (f) of 4 mm, an image size of 1,280 × 1,024 pixels, a sensor size of 6.144 mm × 4.9152 mm, and a pixel size of 0.0048 mm. Camera calibration was performed by simulating the acquired image datasets after establishing the test-bed and initial internal and external orientation parameters to estimate the internal orientation parameters and evaluate their accuracy. The following figures illustrate the detection and labeling results of targets during the simulation process (Figures 6).

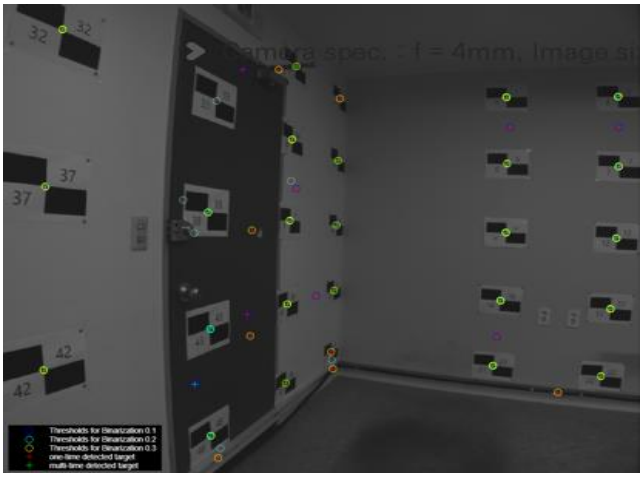

Figure 6. Detection and labeling results of targets

The calculated internal and external orientation parameters (IOPs/EOPs) and their accuracy from the camera calibration experiment are presented in Table 2. At that time, the overall RMSE of camera calibration was 0.392 pixel.

Table 2. Calculation results of IOPs

	x_p	y_p	f	K_1	K_2	K_3	P_1	P_2	A_1	A_2
Calculated IOPs (mm)	-0.056	-0.071	4.091	-0.016	0.0	0.000011	0.0	0.000089	0.000047	-0.00004
Calculated IOPs (pixel)	-11.601	-14.714	852.304	-0.016	0.0	0.000011	0.0	0.000089	0.000047	-0.00004
STD (pixel)	0.003	0.003	0.002	0.000	0.000046	0.000003	0.000094	0.000086	0.0	0.0

In the process of calculating IOPs/EOPs using the camera model equation, correlations between variables may occur. This correlation analysis between variables is performed by partially differentiating each variable in the camera model equation. During this process, variables may converge to or diverge from a local optimum solution, potentially reducing calibration accuracy. In general, calibration methods based on tie points, such as those used in this experiment, are known to have high correlations between variables like the A-A pair (Habib and Morgan, 2003). In this camera calibration experiment, it was analyzed that there was almost no correlation between major internal and external variables (Table 3). However, similar to Habib and Morgan's (2003) research results, strong negative correlations were found between the K_1-K_2, K_2-K_3 pair (−0.964, −0.983), and strong positive correlations were observed between the K_1-K_3pair (0.907).

Table 3. Correlation analysis results between IOPs and EOPs

	x_p-X_0	y_p-Y_0	f-Z_0	x_p-ϕ	y_p-ω	X_0-ϕ	Y_0-ω
Correlation values	0.186	0.290	0.260	0.434	0.465	0.250	0.123

3.3 System Calibration Experimental Results

System calibration was performed by inputting the internal orientation parameters calculated during the camera calibration as initial values. After entering the ground control points (GCPs) and external orientation parameters calculated from the camera calibration, patches were detected and extracted, and then labeled and assigned coordinate values for each patch plane (Figure 7).

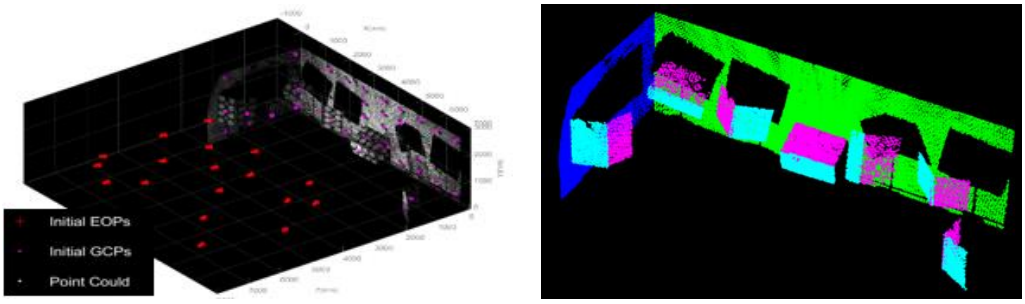

Figure 7. Simulation process for system calibration (left: initial values setting-up, right: patches extraction of V-type targets)

The relative orientation parameters (ROPs) were estimated by simulating the acquired images and LiDAR datasets, using the internal and external orientation parameters obtained from the camera calibration as initial values. The accuracy of these estimates was then evaluated. Table 4 shows the results of the system calibration simulation, including the calculated relative orientation parameters between sensors and their standard deviations. The positional error was found to be 3−5 mm, and the sensor attitude error was 0.001˚, with an RMSE of about 0.2 pixels, indicating that the calibration was generally performed with high accuracy.

Table 4. Simulation results of ROPs between LiDAR scanner and camera

	X_0	Y_0	Z_0	ω	ϕ	x
Calculated ROPs (mm)	0.017	0.110	0.011	-0.826	2.321	1.873
STDV (mm)	5.4	5.496	3.497	0.001	0.001	0.001

The analysis results of correlations between the relative orientation parameters (ROPs) of the sensors presents show while strong negative correlations were observed between the A-A pair, the correlations among the other parameters were relatively low. Figure 8 shows the accurately estimated positions of the robot and targets after system calibration.

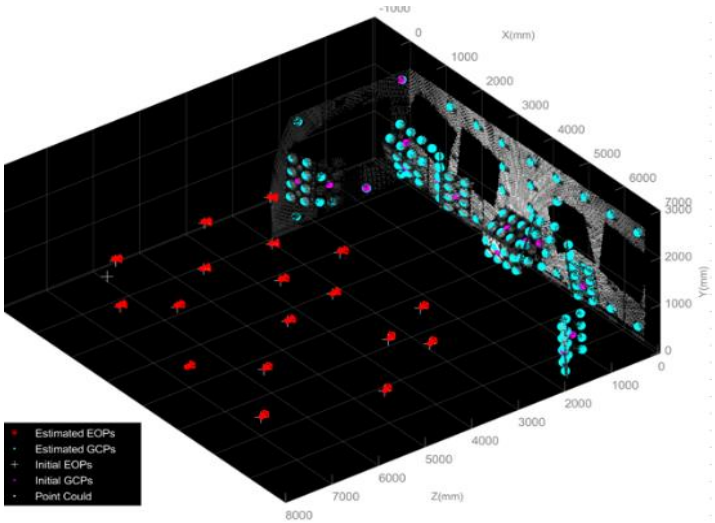

Figure 8. Simulation results of system calibration

The Figure 9 illustrates the fused LiDAR point cloud data with the RGB images obtained from the camera after system calibration. The image indicates that the two datasets were qualitatively well integrated.

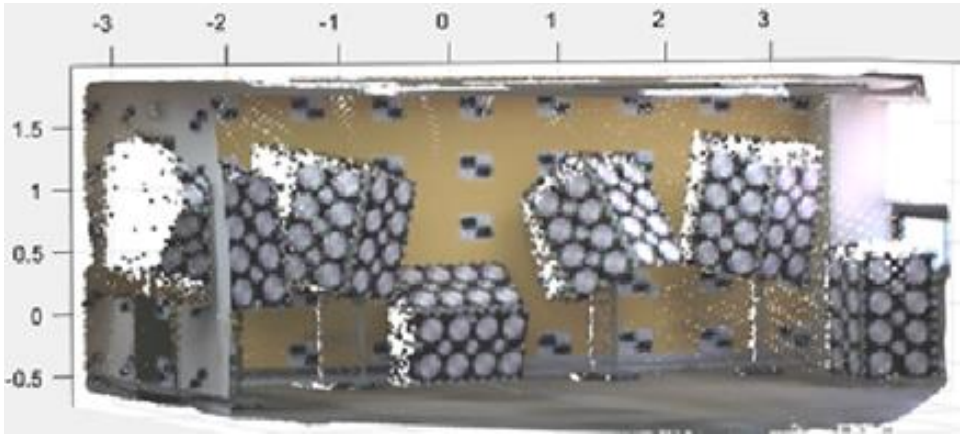

Figure 9. Fused LiDAR data and RGB imagery after system calibration

The results of the system and camera calibration experiments indicate that they can be utilized to improve the SLAM accuracy of survey robots in indoor environments, and to detect and analyze disaster information in indoor environments more accurately and precisely.

4. Conclusions

In order to objectively identify the causes of recent natural disasters and investigate accident sites, the National Disaster Management Research Institute (NDMI) is developing a ground disaster investigation robot (iRobot Packbot) to investigate disaster sites such as earthquakes and structural collapses, where access by investigators is difficult, for tasks such as disaster information detection and collapse risk assessment.

The camera and system calibration process is an essential pre-processing step for ensuring the accuracy of the LiDAR/Vision-based Simultaneous Localization and Mapping (SLAM) module. Firstly, camera calibration estimates the interior orientation parameters (IOPs). Additionally, system calibration calculates the relative positions and attitudes of individual

sensors which constitute the multi-sensor module of the investigation robot, geometrically enhancing the overall observation accuracy of the system.

Experiments for camera and system calibration were conducted by placing wall targets and V-shaped three-dimensional calibration boards in indoor spaces and acquiring images and point clouds for various experimental conditions. Considering the field of view between the camera and LiDAR, camera resolution, distance, and indoor illumination, the characteristics of noise generation in the LiDAR point cloud were confirmed. For system calibration of the multi-sensor module, images and point clouds for the V-shaped three-dimensional calibration board were obtained from 9 locations at a rate of 20 shots per second, while for camera calibration, image data for flat calibration boards on walls were obtained from 6 locations, considering distance and height variations.

The results of camera and system calibration showed precise experimental outcomes, with the camera IOP estimation error (RMSE) through the calibration experiment being 0.39 pixels and the system calibration between LiDAR and camera showing errors within 0.2 pixels. Based on the experimentally derived system and camera calibration results, it is anticipated that the enhanced SLAM accuracy of future investigation robots in indoor spaces and more precise and accurate detection and analysis of indoor disaster information could be achieved.

Acknowledgement

This research outputs are the part of the project "Disaster Field Investigation using Mobile Robot technology (Ⅳ)", which is supported by the NDMI (National Disaster Management Research Institute) under the project number NDMI-MA-2024-06-02. The authors would like to acknowledge the financial support of the NDMI.

References

Choi, K. H., Y. Kim, & C. Kim, (2019), Analysis of Fish-Eye Lens Camera Self-Calibration. *Sensors 2019*, 19, 1218. https://doi.org/10.3390/s19051218

Choi, K. H., & Kim, C. (2022), A Framework of Wearable Sensor-System Development for Urban 3D Modeling, *Applied Science*, 9061. https://doi.org/10.3390/app12189061

Do. L. G., Kim. C. J., & Kim. H. S., (2020) Improved Georeferencing of a Wearable Indoor Mapping System Using NDT and Sensor Integration, *Journal of the Korean Society of Surveying, Geodesy, Photogrammetry and Cartography*, Vol. 38, No. 5, 425-433. https://doi.org/10.7848/ksgpc.2020.38.5.425

Habib, A. F., M. F. Morgan, Automatic calibration of low-cost digital cameras, *Optical Engineering* Vol. 42, No. 4, (1 April 2003). https://doi.org/10.1117/1.1555732

Kim, S., Suk, J., Jung, Y., Lim, E., Koo, S., Kim, C., Choi, K. (2024), System Calibration of a Ground Robot for Disaster and Accident Field Investigation, *2023 KSGPC International Annual Conference, 25-27 April 2024, Pukyong National Univ., Busan, Korea.*

Kim, S., Shin, D., Cho. S., and Kim H., (2021), Development Of A Disaster Robot For Field Investigation Of Building Collapse, *KSCE 2021 Convention Conference & Civil Expo, 20-22 October 2021, GwangJu, Korea.*

NDMI, (2022), Study on Improving Disaster Site Mapping Performance of Multi-sensors based Disaster Investigation Robot, 2022

NDMI, (2023), Study on Field Operation for Disaster Site Investigation through Integration of Investigation Robots and Drones Technology, 2023

Water Journal, Site of heavy rain damage in 2023, Retrieved September 12, 2024, from https://www.waterjournal.co.kr/news/articleView.html?idxno=69346

Wikipedia, Heavy rains on the Korean Peninsula in the summer of 2023, Retrieved September 12, 2024, from https://ko.wikipedia.org/wiki/